Quantitative proteomics study on the protective mechanism of phlorizin on hepatic damage in diabetic db/db mice

WEI-DA LU, BAO-YING LI, FEI YU, QIAN CAI, ZHEN ZHANG, MEI YIN and HAI-QING GAO

Key Laboratory of Cardiovascular Proteomics of Shandong University, Department of Geriatrics, Qi-Lu Hospital of Shandong University, Jinan, Shandong, P.R. China

Received January 4, 2012; Accepted February 16, 2012

DOI: 10.3892/mmr.2012.803

Abstract. Although phlorizin has been used in the treatment of diabetes mellitus for over 100 years, the underlying molecular mechanisms have not been fully elucidated. This study investigated the effect of phlorizin on body weight, blood glucose, blood triglycerides (TG), blood total cholesterol (TC), as well as overall changes in protein expression in db/db diabetic mouse liver. Phlorizin significantly decreased body weight gain and the levels of glucose, TC and TG in blood. Isobaric tag for relative and absolute quantitation (iTRAQ) quantitative proteomics profiling revealed that phlorizin interfered with the processes of carbohydrate metabolism, fatty acid biosynthesis and β-oxidation, cholesterol biosynthesis, and free radical scavenging by affecting the expression of key proteins in these processes. Ingenuity Pathway Analysis successfully established several pathway networks, in which many differentially expressed proteins were involved. The differential expression of several proteins was validated by western blotting. Our study offers important information on the mechanism of phlorizin treatment in diabetes mellitus, particularly in the liver.

Introduction

Type 2 diabetes is one of the most common endocrine diseases in developed countries, which is caused by absolute or relative deficiencies in insulin secretion or insulin action (1). Chronic hyperglycemia is the major biochemical alteration in type 2 diabetes. Moreover, individuals with type 2 diabetes usually display a marked disruption of lipid metabolism, with an abnormal accumulation of fat in various tissues including the liver (2). Hyperglycemia and hyperlipidemia not only impair β-cell function and increase insulin resistance in peripheral tissues, such as the muscle, liver, and adipose tissue (3,4), but also induce oxidative stress reactions, which cause initiation and progression of diabetes-related diseases (5,6). Consequently, regulation of dyslipidemia and reduction in oxidative stress have been regarded as important treatment methods for alleviating diabetes and its complications.

Phlorizin (glucose,1-[2-(β.D-glucopyranosyloxy)-4,6-dihydroxyphenyl]-3-(4-hydroxyphenyl)-1-propanone) is a member of the chalcone class of organic compounds and is mainly distributed in the plants of the genus *Malus* (7). Phlorizin has multiple pharmacological activities, such as anti-oxidative, estrogenic and anti-estrogenic activities, memory improvement and cardioprotective activities (8-11). Reports show that phlorizin inhibits intestinal glucose uptake and renal glucose reabsorption by inhibiting the sodium D-glucose cotransporter (10,12). Phlorizin has been reported to normalize the effects of insulin on glucose metabolism in the liver and other peripheral tissues (13). However, little is known regarding the effect of phlorizin on hepatic damage associated with type 2 diabetes.

The rapidly emerging field of quantitative proteomics provides a powerful technique – isobaric tag for relative and absolute quantitation (iTRAQ) labeling combined with liquid chromatography-tandem mass spectrometry (LC-MS/MS), for the identification and characterization of protein profiles. This technique can lessen variation, enhance throughput and enable quantitative analysis (14).

The aim of the present study was to further clarify the mechanisms of phlorizin in regards to lipid metabolism and oxidative stress in the liver in type 2 diabetes. The well-established C57BLKS/J db/db diabetic mouse was used as the experimental model, which exhibits marked obesity, hyperglycemia and hyperlipidemia that closely resemble those found in human diabetes (15,16). We adopted iTRAQ-LC-MS/MS to investigate the global protein expression changes in the livers of diabetic db/db mice treated with or without phlorizin. Notably, phlorizin treatment ameliorated oxidative stress and metabolic disorders, including hyperlipidemia as well as hyperglycemia.

Materials and methods

Experimental animals and treatment. Male C57BLKS/J db/db and age-matched db/m mice (n=24, 7 weeks of age)

Correspondence to: Dr Hai-Qing Gao, Key Laboratory of Cardiovascular Proteomics of Shandong University, Department of Geriatrics, Qi-Lu Hospital of Shandong University, 107 Wenhuaxi Road, Jinan, 250012 Shandong, P.R. China
E-mail: haiqinggao@yahoo.cn

Key words: type 2 diabetes, db/db mouse, phlorizin, isobaric tag for relative and absolute quantitation proteomics, lipid metabolism, oxidative stress

were purchased from the Model Animal Research Center of Nanjing University (Jiangsu, China). The animals were housed in wire-bottomed cages in a constant environment (room temperature 22±1.6˚C, room humidity 55±5%) with a 12-h light, 12-h dark cycle and received normal pellet chow and tap water *ad libitum*. The mice were kept under observation for one week prior to the start of the experiments. All procedures were approved by the Animal Ethics Committee of Shandong University. C57BLKS/J db/m mice were selected as the control group (n=8). The db/db mice were randomly divided into two groups: the vehicle-treated diabetic group (DM, n=8) administered normal saline solution and the other diabetic group treated with phlorizin (purity >98%, part no. 1005004-19; Jianfeng Inc, Tianjin, China) at a dosage of 20 mg/kg (DMT, n=8). Phlorizin was administered in normal saline solution by intragastric administration for 10 weeks. Each group of mice was observed without any administration of other hypoglycemic therapy throughout the experiment. At the end of the intervention, all mice were fasted overnight and then sacrificed. Fasting blood was collected, and the liver tissue was dissected. The tissues and sera were kept at -80˚C until further analysis.

Measurement of body weight, blood glucose, triglycerides and total cholesterol. Animals were weighed every week. The levels of fasting blood glucose (FBG), blood triglycerides (TG) and blood total cholesterol (TC) were determined using DVI-1650 Automatic Biochemistry and Analysis Instrument (Bayer, Germany) at the end of the treatment.

Histological examination. The excised parts of the livers were immediately fixed in 4% paraformaldehyde and embedded in paraffin. After solidification, 5-μm sections were cut from the blocks. After hematoxylin and eosin (H&E) staining, the sections were examined using light microscopy.

Sample preparation for iTRAQ proteomics. Approximately 50 mg liver tissue from each of four mice from each group was pooled and homogenized in the presence of liquid nitrogen, and then lysed with 500 μl STD buffer (4% SDS, 100 mM DTT, 150 mM Tris HCl pH 8.0). After boiling in water for 5 min, the suspensions were sonicated using an ultrasonic cell crusher for 6 min (10 times, 80 W, 10 sec each time with a 15-sec interval). Then the mixture was incubated again at 100˚C for 5 min. The crude extract was clarified by centrifugation at 14, 000 x g for 20 min.

Trypsin digestion. Proteins (120 μg) for each sample were incorporated into 30 μl STD buffer, incubated in boiling water for 5 min, cooled to room temperature, diluted with 200 μl UA buffer (8 M urea, 150 mM Tris HCl, pH 8.0) and transferred to 30-kDa ultrafiltration. The samples were centrifuged at 14,000 x g for 15 min and then 200 μl UA buffer was added. The samples were centrifuged for 15 min at the same conditions. After that, 100 μl 50 mM iodoacetamide in UA buffer was added, and the samples were incubated for 20 min in darkness. After a 10-min centrifugation at the above conditions, the filters were washed three times with 100 μl UA buffer. Subsequently, 100 μl DS buffer (50 mM triethylammonium bicarbonate at pH 8.5) was added to the filters, and the samples were centrifuged for 10 min at the same conditions as before. This step was repeated twice. Finally, 2 μg trypsin (Promega) in 40 μl DS buffer was added to each filter. The samples were incubated overnight at 37˚C. The resulting peptides were collected by centrifugation. The filters were rinsed with 40 μl 10X DS buffer.

iTRAQ labeling and strong cation exchange separation. Concentration of the peptides was measured by a UV spectrometer using 0.1% solution of vertebrate proteins as the standard (OD 1.1 at 280 nm). Approximately 60 μg peptides of each group was labeled with iTRAQ reagents (114 for the peptides of the control group, 116 for the peptides of the DMT group, and 117 for the peptides of the DM group) following the manufacturer's instructions (Applied Biosystems).

The labeled samples were dried and diluted with 20 vol of cation exchange binding vuffer (10 mM KH_2PO_4 in 25% acetonitrile at pH 3.0). Strong cation exchange (SCX) chromatography was performed to separate the labeled samples into 10 fractions by polysulfoethyl A column (4.6 μm x 100 mm, 200 Å, PolyLC). A suitable gradient elution was applied to separate the peptides at a flow rate of 1 ml/min with elution buffer (10 mM KH_2PO_4, 500 mM KCl in 25% acetonitrile at pH 3.0). Eluted peptides were collected and desalted by an offline fraction collector and C18 cartridges (Sigma).

Mass spectrometric analysis of iTRAQ samples. Mass spectrometric analysis was performed using a micro-liquid chromatography system (MDLC, GE Healthcare) and a (linear trap quadrupole) LTQ-Velos ion trap mass spectrometer (ThermoFinnigan, San Jose, CA, USA). The separation column was a 0.15 mm x 150 mm capillary packed with Zorbax 300SB-C18 particles (Agilent Technologies). Mobile phase A (0.1% formic acid in water) and mobile phase B (0.1% formic acid in ACN) were selected. The volumetric flow rate in the separation column was set to ~1 μl/min, with a 100-min separation gradient running from 0 to 50% B.

MS data were acquired using data-dependent acquisition conditions; each MS event was followed by zoom/MS^2 scans on the five top-most intense peaks; zoom scan width was ±5 m/z; dynamic exclusion was enabled at repeat count 1, repeat duration 30 sec, exclusion list size 200, exclusion duration 60 sec, and exclusion mass width ±1.5 m/z. Pulsed Q (collision induced) dissociation (PQD) parameters were set at isolation width 2 m/z, normalized collision energy 35%, activation Q 0.7, and activation time 0.1 msec; the threshold for MS/MS acquisition was set to 500 counts.

Data analysis. For protein identification and statistical validation, the acquired MS/MS spectra were automatically searched against the non-redundant International Protein Index (IPI) mouse protein database (version 3.72) using the Turbo SEQUEST program in the BioWorks™ 3.1 software suite. The database search parameters included the following settings: the number of allowed missed tryptic cleavage sites was set to 2, the peptide tolerance was 2 Da, the fragment ion tolerance was 1 Da, and only fully tryptic fragments were considered for peptide selection. The sensitivity threshold and mass tolerance for extracting the iTRAQ ratios were set to 1 and ±0.5, respectively. Data filtering parameters were chosen

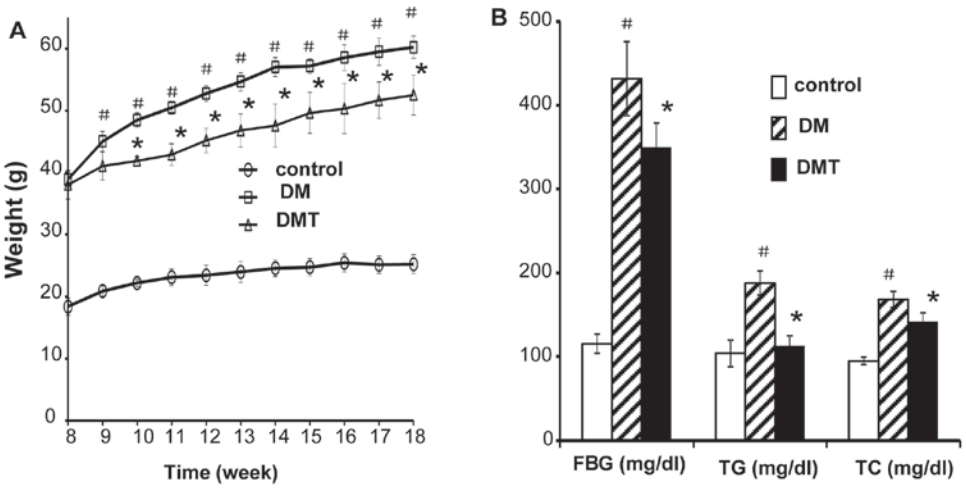

Figure 1. General characteristics. (A) Weight change of the mice in the control, DM and DMT groups. (B) Measurement of FBG, TG and TC 10 weeks after initiation of the experiment. Error bar, standard deviation. *P<0.05, significant difference between the DMT and DM group; #P<0.05, significant difference between the control and DM group (n=8). DM, vehicle-treated diabetic group; DMT, diabetic group treated with phlorizin at a dosage of 20 mg/kg. FBG fasting blood glucose; TG, triglycerides; TC, total cholesterol.

to generate false-positive protein identification rates of <1%, as calculated by searching the MS^2 scans against a forward reversed database of proteins. A threshold was set to 1.5 with a P-value <0.05 yielding at least a 50% change in abundance compared to the reference (control group).

Protein pathway analysis. The differentially expressed genes were analyzed through the use of Ingenuity Pathway Analysis (IPA, Ingenuity Systems, www.ingenuity.com). The data set that contained the differentially expressed proteins identified in the iTRAQ experiment was converted by IPA to 'fold change' and uploaded into IPA. Each identifier was mapped to its corresponding gene object in the Ingenuity Pathways Knowledge Base. These genes, called focus genes, were overlaid onto a global molecular network developed from information contained in the Ingenuity Pathways Knowledge Base. Networks of these focus genes were then algorithmically generated based on their connectivity.

The molecular interactions between genes/gene products were generated as graphical representations. The nodes represent genes or gene products, and the edge represents the biological relationship between two nodes. The intensity of the node color indicates the abundance and the various shapes of the nodes represent the molecular class of the gene product.

Western blot analysis. The western blot procedure was previously described (17). In brief, pooled total proteins (40 μg) from four mice in each group were subjected to gel electrophoresis. The proteins were then transferred onto a polyvinylidene difluoride (PVDF) membrane (Millipore, Bedford, MA, USA). After the membrane was blocked in 5% non-fat dry milk in Tris-buffered saline for 1 h at room temperature, it was incubated with the primary antibody at 4˚C overnight. Subsequently, the blot was incubated with peroxidase-conjugated secondary antibodies at room temperature for at least 1 h and was visualized with enhanced chemiluminescence (ECL) detection system. (Amersham Pharmacia Biotech, Buckinghamshire, UK). Anti-acetyl-CoA carboxylase α (ACACA) and anti-catalase (CAT) (1:1000) primary antibodies were obtained from Cell Signaling (Beverly, MA, USA). Anti-3-hydroxy-3-methylglutaryl-CoA synthase 2 (HMGCS2) and anti-NAD(P)-dependent steroid dehydrogenase-like (NSDHL) (1:1000) primary antibodies were obtained from Abcam (Cambridge, MA, USA). Anti-β-actin (1:5,000) was obtained from Sigma-Aldrich (MA, USA) and served as the loading control.

Statistical analysis. Statistical analysis was performed using SPSS 16.0. One-way ANOVA was applied with Tukey's post hoc test for multiple comparisons.

Results

General characteristics. As shown in Fig. 1A, the initial, final, and gain in body weight in the DM group were significantly higher than those values in the control group. However, the body weight gain was significantly inhibited from the second week after phlorizin administration in the DMT group compared to the DM group.

Fig. 1B shows the levels of serum FBG, TG and TC. The levels of FBG, TG and TC in the DM group were markedly elevated compared with the levels in the control group. Moreover, these three parameters were significantly decreased by 10 weeks of phlorizin administration in the DMT group when compared with the DM group.

Histological examination. In order to ascertain whether phlorizin has any beneficial effect on hepatocellular damage in db/db mice, the liver sections were examined by H&E staining after 10 weeks of treatment. As shown in Fig. 2, the degree of hepatocellular damage was higher in the livers of the DM group than that of the control group. Yet, phlorizin treatment significantly ameliorated the hepatocellular damage in DMT group.

iTRAQ proteomics profiling on the effect of phlorizin in db/db mouse liver. Protein profiling was analyzed using iTRAQ

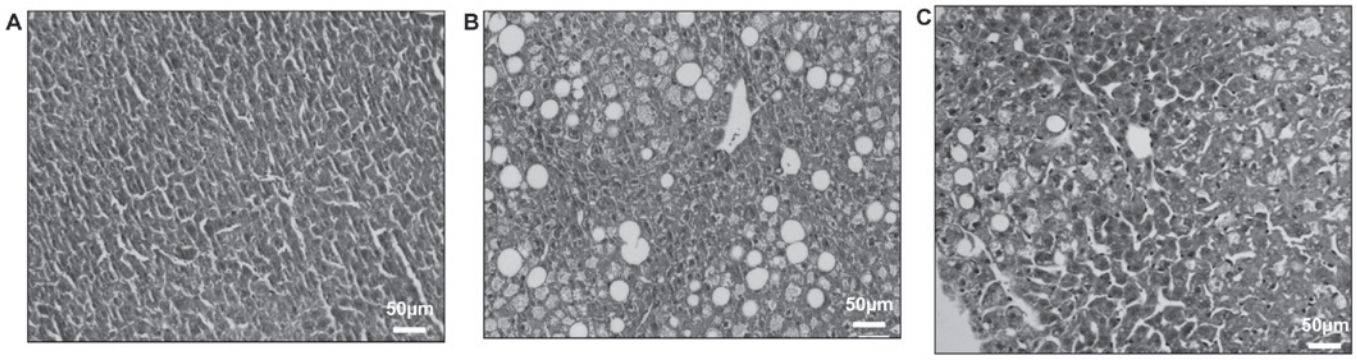

Figure 2. H&E staining of hepatic tissue 10 weeks after initiation of the experiment. (A) Control group, (B) DM group, (C) DMT group. Phlorizin significantly ameliorated the hepatocellular damage in the DMT group. Magnification, x200. DM, vehicle-treated diabetic group; DMT, diabetic group treated with phlorizin at a dosage of 20 mg/kg.

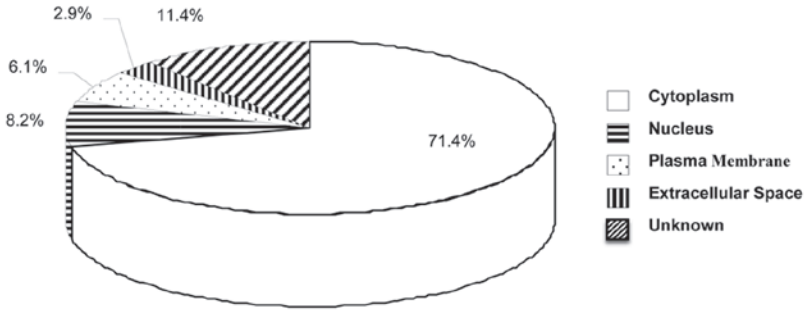

Figure 3. Cellular distribution of the differentially expressed proteins from the iTRAQ experiment, which was analyzed with Ingenuity Pathway Analysis (IPA) software.

approach. A total of 1821 proteins were identified. A strict cutoff value of a 1.5-fold change was used for identification of differential proteins. The false-positive rate was set at <1% to guarantee the accuracy of results. Two hundred and fifteen proteins were elevated in the DM group compared with the control group and were then inhibited by phlorizin treatment. Forty-six proteins were inhibited in the DM group compared with control group and then restored by phlorizin treatment. Ingenuity Pathway Analysis with all 261 differentially expressed proteins showed that 71% were from the cytoplasm, 8% were from the nucleus, 6% were from the plasma membrane, 3% were from the extracellular space, and 11% of the proteins are uncategorized (Fig. 3).

Gene Ontology studies using Ingenuity Pathway Analysis software classified the significantly altered proteins based on their molecular function (Fig. 4A) as well as ranked them based on their biological functions. Notably, the top-ranked biological functions included lipid metabolism and free radical scavenging (Fig. 4B), which was consistent with the biological function of phlorizin.

Fig. 5 documents the top two protein networks generated by the pathway analysis of the differentially expressed proteins. Network A consisted of a cluster of 35 proteins, of which 25 were included in our list. This network had a score of 46 and consisted of proteins involved in lipid metabolism, small molecule biochemistry, and molecular transport. ACACA, acetyl-CoA carboxylase-β (ACACB), fatty acid synthase (FASN), malic enzyme 1 (ME1), carnitine palmitoyltransferase 1A (CPT1A), CAT, glutathione peroxidase 1 (GPX1), glutathione peroxidase 4 (GPX4) and superoxide dismutase 2 (SOD2) were all included in this protein network. Network B consisted of a cluster of 30 proteins, of which 16 were included in our list. This network had a score of 42 and consisted of proteins involved in lipid metabolism, energy production and small molecule biochemistry. Oxoglutarate dehydrogenase-like (OGDHL), 2-oxoglutarate dehydrogenase complex component E2 (DLST), HMGCS2, farnesyl diphosphate synthase (FDPS), lanosterol synthase (LSS) and fatty acid desaturase 1 (FADS1), were included in this protein network. This result prompted us to further explore the relationship among fatty acid biosynthesis and β-oxidation, cholesterol synthesis and oxidation stress.

Relevance of iTRAQ data set proteins to the process of metabolic disorders in db/db mouse liver. The altered proteins from the iTRAQ experiment were functionally analyzed to clarify the molecular events involved in the pathophysiological mechanisms of metabolic disorders in type 2 diabetes. Proteins from different classes are described below.

Alterations in carbohydrate metabolism. The combination of enhancement in glycolysis and suppression in acetyl-CoA oxidation leads to accumulation of mitochondrial acetyl-CoA, which can be transported into the cytosol and utilized for *de novo* biosynthesis of fatty acids and cholesterol. Several of the key enzymes involved in these pathways, which were

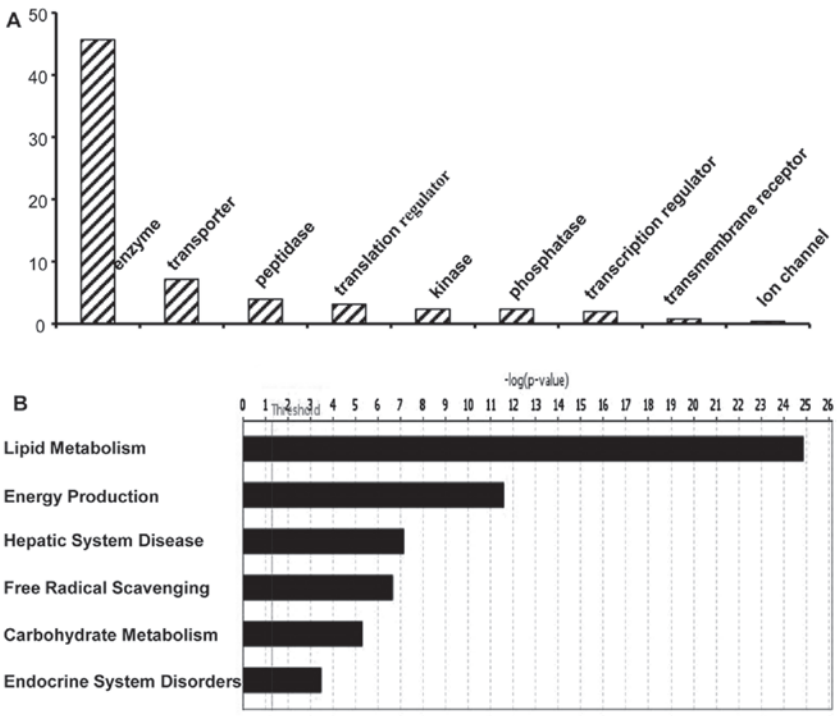

Figure 4. Ingenuity Pathway Analysis (IPA) for differentially expressed proteins. (A) Categorization of significantly regulated proteins based on their molecular functions. (B) Top bio-functional processes, with which the differentially expressed proteins are associated. Lipid metabolism is the most significant process.

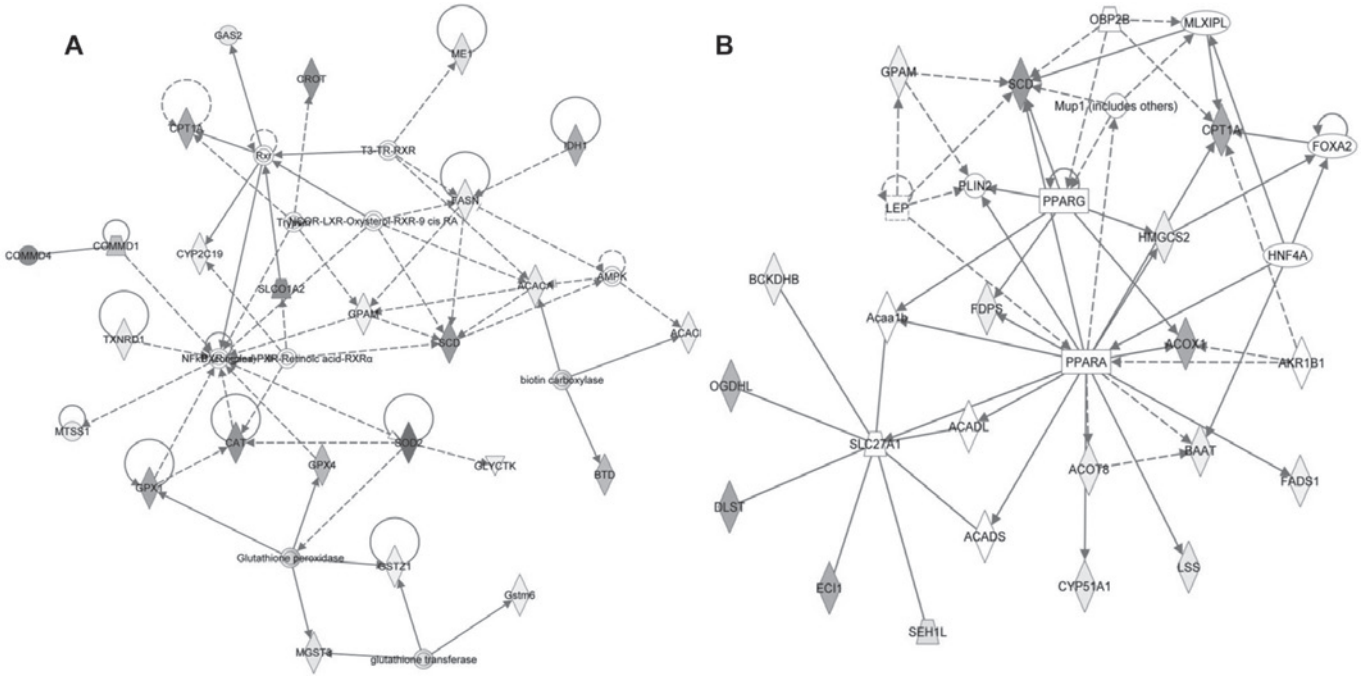

Figure 5. Top two networks, in which differential proteins are likely to be involved. (A) Network for lipid metabolism, small molecule biochemistry, and molecular transport. (B) Network for lipid metabolism, energy production, and small molecule biochemistry.

dysregulated in the DM group, were reversed by phlorizin treatment. As shown in Table I, 6-phosphofructokinase (PFKL) and pyruvate kinase isozymes M1/M2 (PKM2), the key-limiting enzymes in glycolysis, were down-regulated to 0.50- and 0.36-fold in the DMT group compared to the DM group, indicating inhibition of the liver glycolytic pathway. Pyruvate, the product of glycolysis, is converted to acetyl-CoA through the action of pyruvate dehydrogenase (PDH). PDH complex component E2 (DLAT) was down-regulated in the DMT group compared to the DM group. Meanwhile, the key enzymes involved in the TCA cycle were up-regulated in the DMT group, including citrate synthase (CS), isocitrate

Table I. Functional classification of the altered proteins related to carbohydrate metabolism.

Accession no.	Symbol	Entrez gene name	Unique peptide	Cover percent	iTRAQ ratio			
					116:114	117:114	116:117	
Glycolysis								
IPI00387312	PFKL	Phosphofructokinase, liver	2	3.7	1.55	3.09	0.50	↓
IPI00845840	PKM2	Pyruvate kinase isozymes M1/M2	5	16.2	0.72	2.01	0.36	↓
TCA cycle-related								
IPI00153660	DLAT	Pyruvate dehydrogenase complex component E2	6	13.6	1.09	1.81	0.60	↓
IPI00113141	CS	Citrate synthase	8	22.8	1.12	0.43	2.61	↑
IPI00845858	DLST	2-oxoglutarate dehydrogenase complex component E2	4	27.4	1.33	0.55	2.42	↑
IPI00762452	IDH1	Isocitrate dehydrogenase 1 (NADP), soluble	21	59.2	1.72	0.77	2.23	↑
IPI00342603	OGDHL	Oxoglutarate dehydrogenase-like	4	4.7	1.84	0.93	1.98	↑
IPI00406442	SUCLG1	Succinate-CoA ligase, α subunit	5	21.7	1.52	0.87	1.75	↑

114, control group; 116, DMT group; 117, DM group.

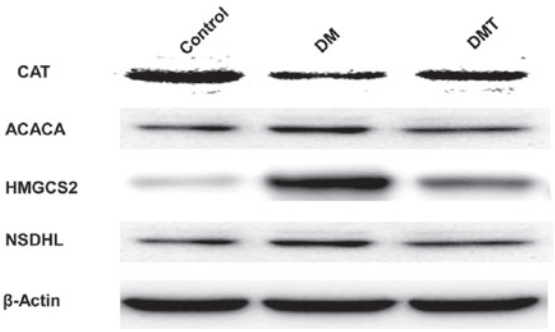

Figure 6. Western blot validation for four differentially expressed proteins: CAT, ACACA, HMGCS2 and NSDHL. β-actin was used as the loading control. DM, vehicle-treated diabetic group; DMT, diabetic group treated with phlorizin at a dosage of 20 mg/kg.

dehydrogenase 1 (IDH1) and DLST, indicating the reduction in the amount of acetyl-CoA.

Alterations in lipid metabolism. The fatty acid biosynthesis pathway appeared to be down-regulated in the DMT group (Table II). The rate-limiting enzymes for fatty acid biosynthesis, ACACA and ACACB, which catalyze the synthesis of malonyl-CoA from acetyl-CoA, were down-regulated to 0.43- and 0.53-fold, respectively, in the DMT group compared to the DM group. FASN, which catalyzes the synthesis of palmitate from acetyl-CoA and malonyl-CoA, was also down-regulated to 0.55-fold. Other important enzymes that were down-regulated include: ME1, which catalyzes cytosolic malate to pyruvate in the citrate-pyruvate cycle; FADS1, which catalyzes biosynthesis of highly unsaturated fatty acid; and *trans*-2-enoyl-CoA reductase (MECR). However, elongation of very long chain fatty acid protein 2 (ELOVL2), which catalyzes the synthesis of polyunsaturated very long chain fatty acid, and acyl-CoA desaturase 1 (SCD1), which catalyzes the first step in the synthesis of oleate from stearate were up-regulated in the DMT group.

Fatty acids are catabolized into acetyl-CoA mainly through β-oxidation in mitochondria (Table II). In the DM group, several enzymes involved in fatty acid β-oxidation were down-regulated. Part of the inhibition was reversed by phlorizin administration. The rate-limiting step for β-oxidation is to activate long chain fatty acid transportation into the mitochondria by CPT1A, which was up-regulated by 2.32-fold in the DMT group compared to the DM group. 3,2-*trans*-enoyl-CoA isomerase (DCI), which is essential for the degradation of unsaturated fatty acids, was also up-regulated by 2.26-fold. Another mode of β-oxidation is for fatty acids longer than 22 carbons, which is first shortened in peroxisomes before being catabolized into acetyl-CoA in the mitochondria. Several peroxisome β-oxidation enzymes, such as carnitine *O*-octanoyltransferase (CROT), acyl-coenzyme A oxidase 1 (ACOX1), hydroxysteroid (17-β) dehydrogenase 4 (HSD17B4) and 2-hydroxyacyl-CoA lyase 1 (HACL1), were up-regulated in the DMT group. On the other hand, acyl-CoA thioesterase 1 (ACOT1), which catalyzes the hydrolysis of acyl-CoAs, highly specific for saturated long chain fatty acids, was down-regulated in the DMT group. 2,4-Dienoyl CoA reductase 2 (DECR2), participating in the degradation of unsaturated fatty enoyl-CoA esters in peroxisome, was also down-regulated in the DMT group.

Considering acetyl-CoA is also the substrate for *de novo* cholesterol biosynthesis, we investigated whether this pathway was down-regulated in the DMT group. As shown in Table II, several key enzymes in the cholesterol synthesis pathway, including acetyl-CoA acetyltransferase 2 (ACAT2), HMGCS2, FDPS, NSDHL and LSS, and the enzyme involved in cholesterol esterification, sterol *O*-acyltransferase2 (SOAT2), were all down-regulated in the DMT group compared to the DM group.

Alterations in oxidative stress. Diabetes is usually associated with oxidative stress. As shown in Table III, the key anti-oxidative enzymes appeared to be down-regulated in the DM group but were stimulated again by phlorizin treatment. SOD2, which catalyzes dismutation of superoxide anion into hydrogen peroxide, was increased by 4.19-fold in the

Table II. Functional classification of the altered proteins related to lipid metabolism.

Accession no.	Symbol	Entrez gene name	Unique peptide	Cover percent	iTRAQ ratio			
					116:114	117:114	116:117	
Fatty acid synthesis								
IPI00848443	ACACA	Acetyl-CoA carboxylase α	8	5.4	1.82	4.22	0.43	↓
IPI00421241	ACACB	Acetyl-CoA carboxylase β	5	2.5	1.39	2.59	0.53	↓
IPI00113223	FASN	Fatty acid synthase	21	11.6	2.12	3.84	0.55	↓
IPI00468859	FADS1	Fatty acid desaturase 1	2	9.4	1.12	1.73	0.65	↓
IPI00268157	ELOVL2	Elongation of very long chain fatty acid protein 2	1	5.8	0.75	0.39	1.92	↑
IPI00121276	MECR	Mitochondrial *trans*-2-enoyl-CoA reductase	2	7.8	0.82	1.97	0.42	↓
IPI00886014	ACSS3	Acyl-CoA synthetase short-chain family member 3	3	7.2	1.52	3.03	0.50	↓
IPI00126796	SLC27A4	Solute carrier family 27, member 4	4	9.6	1.36	2.48	0.55	↓
IPI00128389	PTGS1	Prostaglandin-endoperoxide synthase 1	2	4.3	0.73	2.11	0.35	↓
IPI00122327	PLA2G6	Phospholipase A2, group VI	1	2.9	0.94	1.75	0.54	↓
IPI00128857	ME1	Malic enzyme 1	9	23.9	1.14	3.91	0.29	↓
IPI00322530	SCD1	Stearoyl-CoA desaturase 1	3	11.0	1.65	0.59	2.80	↑
IPI00221606	ACNAT1/2	Acyl-coenzyme A amino acid N-acyltransferase 2	7	21.9	1.48	2.36	0.63	↓
Fatty acid β-oxidation								
IPI00880948	ACADSB	Acyl-CoA dehydrogenase, short/branched chain	2	6.7	0.98	0.62	1.58	↑
IPI00170013	ACAD10	Acyl-CoA dehydrogenase family, member 10	8	10.6	1.30	0.45	2.90	↑
IPI00122633	ACSF2	Acyl-CoA synthetase family member 2	13	32.2	1.73	0.87	1.99	↑
IPI00330094	CPT1A	Carnitine palmitoyltransferase 1A	12	23.0	0.86	0.37	2.32	↑
IPI00331692	DCI1	3,2 *trans*-enoyl-Coenyme A isomerase	7	32.9	0.88	0.39	2.26	↑
IPI00120165	CROT	Carnitine O-octanoyltransferase	17	36.8	1.54	0.51	3.03	↑
IPI00115871	ACOT1	Acyl-CoA thioesterase 1	7	27.2	2.17	3.34	0.65	↓
IPI00331628	HSD17B4	Hydroxysteroid (17-β) dehydrogenase 4	30	49.8	1.59	0.55	2.90	↑
IPI00316314	HACL1	2-Hydroxyacyl-CoA lyase 1	24	56.1	1.22	0.41	2.98	↑
IPI00130804	ECH1	Delta(3,5)-delta(2,4)-dienoyl-CoA isomerase	12	49.9	1.49	0.64	2.33	↑
IPI00125325	DECR2	2,4-dienoyl CoA reductase 2, peroxisomal	10	48.0	1.56	2.46	0.63	↓
IPI00127558	ACOX1	Acyl-CoAoxidase 1	27	56.4	1.53	0.67	2.28	↑
IPI00112111	ABCD1	ATP-binding cassette, sub-family D, member 1	11	22.3	2.35	3.85	0.61	↓
Cholesterol synthesis								
IPI00228253	ACAT2	Acetyl-CoA acetyltransferase 2	4	19.4	1.92	4.54	0.42	↓
IPI00120457	FDPS	Farnesyl diphosphate synthase	4	16.4	0.96	1.85	0.52	↓
IPI00420718	HMGCS2	3-hydroxy-3-methylglutaryl-CoA synthase 2	21	53.2	2.24	4.18	0.54	↓
IPI00128692	NSDHL	NAD(P) dependent steroid dehydrogenase-like	3	14.6	1.06	3.76	0.28	↓
IPI00169958	LSS	Lanosterol synthase	4	6.0	1.13	2.94	0.38	↓
IPI00458711	CYP51	Lanosterol 14-α demethylase	7	18.7	1.00	2.64	0.38	↓
IPI00136247	SOAT2	Sterol O-acyltransferase 2	4	8.0	1.16	2.81	0.41	↓

114, control group; 116, DMT group; 117, DM group.

DMT group compared to the DM group. CAT, GPX1, GPX4, peroxiredoxin 3 (PRDX3), which are responsible for hydrogen peroxide catabolism, were also up-regulated between 1.88- and 2.93-fold in the DMT group. Hydroxysteroid (17-β) dehydrogenase 10 (HSD17B10), which is involved in generation of superoxide and hydrogen peroxide, was decreased to 0.66-fold in the DMT group.

Validation of iTRAQ data on selected candidate proteins. Four candidate proteins were validated using western blot analysis. ACACA, HMGCS2 and NSDHL were found to be inhibited whereas CAT was enhanced in the DMT group compared to the DM group (Fig. 6). This result verified the reliability of the iTRAQ results.

Discussion

Type 2 diabetes mellitus results in abnormal metabolism of glucose, TG, TC and other reactive metabolites caused by insulin-resistant and -deficient states (2,18). More TG-rich

Table III. Functional classification of the altered proteins related to oxidative stress.

Accession no.	Symbol	Entrez gene name	Unique peptide	Cover percent	iTRAQ ratio			
					116:114	117:114	116:117	
IPI00869393	CAT	Catalase	29	66.4	1.32	0.45	2.93	↑
IPI00319652	GPX1	Glutathione peroxidase 1	8	43.8	0.91	0.38	2.39	↑
IPI00117281	GPX4	Glutathione peroxidase 4	4	22.8	1.14	0.61	1.88	↑
IPI00116192	PRDX3	Peroxiredoxin 3	5	19.8	0.98	0.37	2.65	↑
IPI00830581	HSD17B10	Hydroxysteroid (17-β) dehydrogenase 10	11	75.5	1.49	2.26	0.66	↓
IPI00830969	ITGB2	Integrin, β 2	2	20.0	0.94	0.58	1.62	↑
IPI00128389	PTGS1	Prostaglandin-endoperoxide synthase 1	2	4.3	0.73	2.11	0.35	↓
IPI00109109	SOD2	Superoxide dismutase 2, mitochondrial	4	23.0	1.09	0.26	4.19	↑
IPI00469251	TXNRD1	Thioredoxin reductase 1	3	10.0	0.83	2.05	0.41	↓
IPI00226356	TTPA	Tocopherol (α) transfer protein	8	46.8	1.91	3.14	0.61	↓

114, control group; 116, DMT group; 117, DM group.

particles are produced from the liver as a result of insulin resistance. The superfluous TGs are stored in non-adipose tissues, which are worsened by the simultaneous presence of hyperglycemia. Subsequently, the decline and apoptosis of β-cells is caused by the formation of lipotoxicity metabolite and aggravation of oxidative stress (19). Thus, the regulation of hyperlipidemia and the reduction in oxidative stress play an important role in the treatment of diabetes and its complications.

In this study, we investigated and observed a significant elevation in serum FBG, TG, TC levels in the DM group compared with these levels in the control group (Fig. 1B). Moreover, the elevated levels were significantly reduced by the oral administration of phlorizin. These results imply that phlorizin prevents diabetic pathological conditions induced by hyperlipidemia through the lowering of TG and TC levels.

Based on the protein expression profiling, enhancement of genes involved in glycolysis and suppression of genes involved in acetyl-CoA oxidation may lead to accumulation of acetyl-CoA, which can result in the elevated levels of substrate in the synthesis of fatty acid and cholesterol. In addition, several key enzymes in the biosynthetic pathways of fatty acids and cholesterol were significantly inhibited by phlorizin while other proteins in the pathway of fatty acid β-oxidation were markedly stimulated by phlorizin (Table II), which may account for the elevated levels of TG and TC in diabetic livers giving rise to hepatic hyperlipidemia.

Among the genes related to fatty acid synthesis, ACACA and FASN are more significant. Acetyl-CoA carboxylase has two isoforms in rodents, ACACA and ACACB, which is a pivotal physiological regulator for both fatty acid synthesis and oxidation. Inhibition of ACACA decreases fatty acid synthesis and helps remedy systemic and tissue hyperlipidemia (20,21). ACAC2-null mice ($ACAC2^{-/-}$) not only have a higher fatty acid oxidation rate, but also lower hepatic steatosis (22). Our data showed that ACACA and ACACB were both down-regulated in the DMT group. FASN is considered to be a determinant of the maximal capacity of a tissue to synthesize long chain fatty acids by *de novo* lipogenesis (23). Patients suffering from non-alcoholic fatty liver disease display an increased expression level of FASN (24). Notable, FASN was also down-regulated in the DMT group, which suggests that phlorizin inhibits the synthesis of fatty acid. (Table II).

Fatty acid degradation occurs primarily via β-oxidation. Our data revealed that the expression levels of enzymes regulating β-oxidation were up-regulated in the DMT group compared with the DM group. Among these enzymes, CPT1A and DCI deserve more attention. CPT1A is one of the three carnitine palmitoyltransferase 1 (CPT1) isoforms expressed in liver. Elevated expression of CPT1A can correct hepatic steatosis by accelerating liver mitochondrial β-oxidation of long-chain fatty acids (25). DCI is essential for the complete degradation of unsaturated fatty acids, which catalyzes the transformation of 3-*cis* and 3-*trans* intermediates arising during the stepwise degradation of all *cis*-, *mono*-, and polyunsaturated fatty acids (26). In the $DCI^{-/-}$ mouse, mitochondrial unsaturated fatty acid β-oxidation is interrupted (27). Up-regulation of DCI by phlorizin may therefore ameliorate hyperlipidemia in diabetic livers.

As cholesterol homeostasis is critical for maintenance of normal cell function, abnormalities of this metabolism can contribute to pathologic processes including diabetic hepatic damage. Among the identified genes related to cholesterol metabolism, ACAT2, HMGCS2, and NSDHL were all down-regulated in the DMT group (Table II). ACAT2 together with HMGCS2 catalyzes the formation of the substrate 3-hydroxy-3-methylglutaryl-CoA (HMG-CoA), which is subsequently changed to mevalonate by HMG-CoA reductase. It is the rate-limiting step in the pathway. Decreased expression of ACAT2 may suppress the biosynthesis of cholesterol, ameliorating hyperlipidemia in type 2 diabetic livers (28,29). NSDHL encodes a 3-β-hydroxysterol dehydrogenase, which is thought to function in the demethylation of sterol precursors in one of the later steps of cholesterol biosynthesis (30). The expression

levels of HMGCS2 and NSDHL were in accordance with the result of the western blot analysis. For the first time, our study found that phlorizin inhibits the genes involved in cholesterol biosynthesis to decrease the accumulation of detrimental cholesterol.

The expression levels of some enzymes involved in these reactions appeared to be controversial, such as ELOVL2, SCD1, ACOT1, DECR2 (Table II). Due to posttranslational modifications, subcellular location and allosteric regulation, changes in protein levels are not always consistent with changes in activities. Further investigation is necessary to accurately clarify the impacts.

Long-term hyperglycemia and hyperlipidemia result in the generation of reactive oxygen species (ROS) and consequently, increase oxidative stress, which is a key pathogenic factor for diabetes mellitus and its complications (31,32). ROS can attack lipids, proteins and nucleic acids simultaneously, causing defective insulin gene expression and insulin secretion as well as changes in cellular structure and function. Ineffective scavenging of free radicals may contribute to tissue injury. Our results showed that the expression levels of antioxidant enzymes, SOD2, CAT, GPX-1 and GPX-4, were all decreased in the DM group, which implied that increased oxidative damage occurred in the DM group, due to an elevation in ROS generation induced by hyperglycemia and hyperlipidemia. However, phlorizin administration exerted its antioxidant activity by decreasing the expression of these enzymes (Table III). This suggests that the administration of phlorizin may be beneficial to alleviate oxidative stress and prevent or ameliorate diabetic symptoms or complications.

In conclusion, for the first time, we established quantitative iTRAQ profiles of global liver proteins in a db/db diabetic mouse model treated with or without phlorizin. Phlorizin ameliorated hyperlipidemia and oxidative stress by affecting the expression of a set of proteins which were involved in carbohydrate metabolism, fatty acid synthesis and β-oxidation, cholesterol biosynthesis, and free radical scavenging in the mouse liver. At the same time, phlorizin successfully decreased body weight, blood glucose, blood TG, and blood TC. Our study provides novel information in regards to the mechanisms of phlorizin on type 2 diabetic hepatic damage. Phlorizin may become an effective therapeutic agent in the treatment of diabetes mellitus, particularly for complications in the liver.

Acknowledgements

This research was supported by the National Natural Science Foundation of China (30873145, 81000340, 81100595), the Outstanding Young Scientist Research Award Fund of Shandong Province (BS2009YY046), the China Postdoctoral Science Foundation (20100471520, 2011M500748) and the Natural Science Foundation of Shandong Province (Y2008C100, ZR2010HQ067). We wish to thank the personnel of the Medical Science Academy of Shandong and the personnel of the Research Center for Proteome Analysis, Shanghai Institute for Biological Sciences, Chinese Academy of Sciences for their technical support. We also thank Professor Jun-Hui Zhen for his advice regarding the proteomics experiment.

References

1. Fagot-Campagna A, Bourdel-Marchasson I and Simon D: Burden of diabetes in an aging population: prevalence, incidence, mortality, characteristics and quality of care. Diabetes Metab 31 Spec No 2: 5S35-35S52, 2005.
2. McGarry JD: Banting lecture 2001: dysregulation of fatty acid metabolism in the etiology of type 2 diabetes. Diabetes 51: 7-18, 2002.
3. LeRoith D: Beta-cell dysfunction and insulin resistance in type 2 diabetes: role of metabolic and genetic abnormalities. Am J Med 113 (Suppl 6A): 3S-11S, 2002.
4. Robertson RP, Harmon J, Tran PO, Tanaka Y and Takahashi H: Glucose toxicity in beta-cells: type 2 diabetes, good radicals gone bad, and the glutathione connection. Diabetes 52: 581-587, 2003.
5. Stumvoll M, Goldstein BJ and van Haeften TW: Type 2 diabetes: principles of pathogenesis and therapy. Lancet 365: 1333-1346, 2005.
6. Prentki M, Joly E, El-Assaad W and Roduit R: Malonyl-CoA signaling, lipid partitioning, and glucolipotoxicity: role in beta-cell adaptation and failure in the etiology of diabetes. Diabetes 51 (Suppl 3): S405-S413, 2002.
7. Gosch C, Halbwirth H and Stich K: Phloridzin: biosynthesis, distribution and physiological relevance in plants. Phytochemistry 71: 838-843, 2010.
8. Rezk BM, Haenen GR, van der Vijgh WJ and Bast A: The antioxidant activity of phloretin: the disclosure of a new antioxidant pharmacophore in flavonoids. Biochem Biophys Res Commun 295: 9-13, 2002.
9. Wang J, Chung MH, Xue B, Ma H, Ma C and Hattori M: Estrogenic and antiestrogenic activities of phloridzin. Biol Pharm Bull 33: 592-597, 2010.
10. Boccia MM, Kopf SR and Baratti CM: Phlorizin, a competitive inhibitor of glucose transport, facilitates memory storage in mice. Neurobiol Learn Mem 71: 104-112, 1999.
11. Gupte A and Buolamwini JK: Synthesis and biological evaluation of phloridzin analogs as human concentrative nucleoside transporter 3 (hCNT3) inhibitors. Bioorg Med Chem Lett 19: 917-921, 2009.
12. Burcelin R, Mrejen C, Decaux JF, De Mouzon SH, Girard J and Charron MJ: In vivo and in vitro regulation of hepatic glucagon receptor mRNA concentration by glucose metabolism. J Biol Chem 273: 8088-8093, 1998.
13. Rossetti L, Smith D, Shulman GI, Papachristou D and DeFronzo RA: Correction of hyperglycemia with phlorizin normalizes tissue sensitivity to insulin in diabetic rats. J Clin Invest 79: 1510-1515, 1987.
14. Ross PL, Huang YN, Marchese JN, *et al*: Multiplexed protein quantitation in *Saccharomyces cerevisiae* using amine-reactive isobaric tagging reagents. Mol Cell Proteomics 3: 1154-1169, 2004.
15. Hummel KP, Dickie MM and Coleman DL: Diabetes, a new mutation in the mouse. Science 153: 1127-1128, 1966.
16. Herberg L and Coleman DL: Laboratory animals exhibiting obesity and diabetes syndromes. Metabolism 26: 59-99, 1977.
17. Li XL, Li BY, Gao HQ, *et al*: Proteomics approach to study the mechanism of action of grape seed proanthocyanidin extracts on arterial remodeling in diabetic rats. Int J Mol Med 25: 237-248, 2010.
18. Scott JA and King GL: Oxidative stress and antioxidant treatment in diabetes. Ann NY Acad Sci 1031: 204-213, 2004.
19. Poitout V and Robertson RP: Minireview: secondary beta-cell failure in type 2 diabetes – a convergence of glucotoxicity and lipotoxicity. Endocrinology 143: 339-342, 2002.
20. Savage DB, Choi CS, Samuel VT, *et al*: Reversal of diet-induced hepatic steatosis and hepatic insulin resistance by antisense oligonucleotide inhibitors of acetyl-CoA carboxylases 1 and 2. J Clin Invest 116: 817-824, 2006.
21. Mao J, DeMayo FJ, Li H, *et al*: Liver-specific deletion of acetyl-CoA carboxylase 1 reduces hepatic triglyceride accumulation without affecting glucose homeostasis. Proc Natl Acad Sci USA 103: 8552-8557, 2006.
22. Abu-Elheiga L, Matzuk MM, Abo-Hashema KA and Wakil SJ: Continuous fatty acid oxidation and reduced fat storage in mice lacking acetyl-CoA carboxylase 2. Science 291: 2613-2616, 2001.
23. Wakil SJ: Fatty acid synthase, a proficient multifunctional enzyme. Biochemistry 28: 4523-4530, 1989.

24. Ouyang X, Cirillo P, Sautin Y, *et al*: Fructose consumption as a risk factor for non-alcoholic fatty liver disease. J Hepatol 48: 993-999, 2008.
25. Akkaoui M, Cohen I, Esnous C, *et al*: Modulation of the hepatic malonyl-CoA-carnitine palmitoyltransferase 1A partnership creates a metabolic switch allowing oxidation of de novo fatty acids. Biochem J 420: 429-438, 2009.
26. Janssen U, Fink T, Lichter P and Stoffel W: Human mitochondrial 3,2-*trans*-enoyl-CoA isomerase (DCI): gene structure and localization to chromosome 16p13.3. Genomics 23: 223-228, 1994.
27. Janssen U and Stoffel W: Disruption of mitochondrial beta-oxidation of unsaturated fatty acids in the 3,2-*trans*-enoyl-CoA isomerase-deficient mouse. J Biol Chem 277: 19579-19584, 2002.
28. Jung UJ, Lee MK, Park YB, Kang MA and Choi MS: Effect of citrus flavonoids on lipid metabolism and glucose-regulating enzyme mRNA levels in type-2 diabetic mice. Int J Biochem Cell Biol 38: 1134-1145, 2006.
29. Park SA, Choi MS, Kim MJ, *et al*: Hypoglycemic and hypolipidemic action of Du-zhong (*Eucommia ulmoides* Oliver) leave water extract in C57BL/KsJ-db/db mice. J Ethnopharmacol 107: 412-417, 2006.
30. Caldas H and Herman GE: NSDHL, an enzyme involved in cholesterol biosynthesis, traffics through the Golgi and accumulates on ER membranes and on the surface of lipid droplets. Hum Mol Genet 12: 2981-2991, 2003.
31. Oberley LW: Free radicals and diabetes. Free Radic Biol Med 5: 113-124, 1988.
32. Baynes JW: Role of oxidative stress in development of complications in diabetes. Diabetes 40: 405-412, 1991.